

9 Louvers

B. E. Hardt,* R. D. Karam,† and R. J. Eby†

Introduction

Louvers are active thermal-control elements that have been used in different forms on numerous spacecraft. While most commonly placed over external radiators, louvers may also be used to modulate heat transfer between internal spacecraft surfaces, or from internal surfaces directly to space through openings in the spacecraft wall.

In general, a louver in its fully open state can reject six times as much heat as it does in its fully closed state, with no power being required to operate it. Thus louvers find application where internal power dissipation varies rather widely as a result of equipment duty cycles. The most commonly used louver assembly is the bimetallic, spring-actuated, rectangular-blade (venetian-blind) type. Hydraulically activated louvers and pinwheel louvers are used less often today than in the past.

Louver reliability can be improved at the design stage by making each louver blade independently actuated by a bimetallic clock spring. Thus a single-point failure is associated with one blade, not the entire assembly. The spring can be integrated with a heater/controller to decrease the passive closed-to-open temperature range of 10–17°C to as little as 1°C.

Louver radiator assemblies (illustrated in Fig. 9.1) consist of five main elements: baseplate, blades, actuators, sensing elements, and structural elements. The baseplate is a surface of low absorptance-to-emittance ratio that covers the critical set of components whose temperature is being controlled. Blades, which are driven by the actuators, are the louver elements that give variable-radiation characteristics to the baseplate. While closed, louvers shield and decouple the baseplate from the surroundings, but while open, they allow a radiative coupling between the baseplate and the surroundings. The radiation characteristics of the baseplate can be varied over the range defined by these two extreme positions.

The actuators drive the blades according to the perceived baseplate temperature. Actuators of louvers flown on satellites have been bimetallic spirals or bellows, although other types of actuators could be used, such as Bourdon spirals and electrical devices. In a single-actuation system, all the blades are driven by a single actuator. In a multiple-actuation system, several actuators are required. Generally, bimetallic devices are used as actuators in multiple-actuation systems, and bellows in single-actuation systems.

The actuator drives the blade angle as determined by the baseplate temperature. A strong conductive path between the actuator and baseplate is therefore sought to minimize the temperature gradient between them. The thermal coupling between a bimetallic actuator and baseplate is composed of both radiative and conductive paths. Bellows and Bourdon actuators use a tank or tube containing liquid or both

*The Aerospace Corporation, El Segundo, California.

†Orbital Sciences Corporation, Dulles, Virginia.

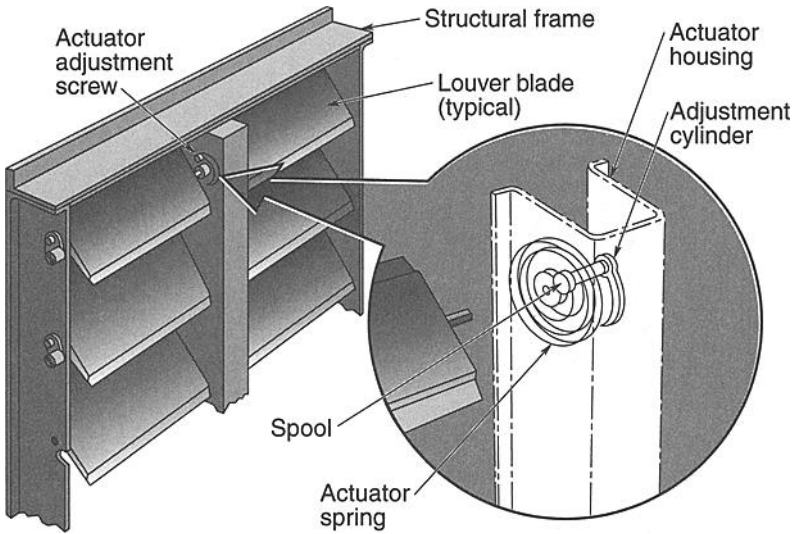


Fig. 9.1. Orbital Sciences louver assembly schematic.

liquid and vapor to actuate the blades. The tank or tube is typically soldered to the baseplate to ensure a strong conductive coupling.

Louver assemblies have been designed for operation in both shadow and sunlight. Two design approaches that have been followed for operation in sunlight are the use of a sun shield and the modification of the louver assembly for high temperature operation.

Vane Louvers

As noted earlier, the most widely used louver assembly is the bimetallic, spring-actuated, rectangular-blade type, known as “venetian-blind” or “vane” louvers. The arrangement of actuators, housing, blades, and structure for a vane louver assembly is shown schematically in Fig. 9.1. Design features vary depending on whether the assembly is to be exposed to solar illumination and whether actuation is to be provided by a bimetallic spring alone or by a bimetallic spring in conjunction with a heater/controller, as well as according to supplier-specific differences. Current principal suppliers are Orbital Sciences Corporation, Swales Aerospace, and Starsys. Characteristics of flight-qualified rectangular-blade louver assemblies are listed in Table 9.1.

In most designs, blade rotation is effected by the expansion or contraction of a spiral bimetallic actuator, by virtue of heat gained or lost in exchange with the equipment-mounting plate (Fig. 9.2). One end of the actuator is attached to the frame structure and the other to the Teflon spool. A square cutout in the spool supports the inboard louver-blade end. The actuator is coated black in order to enhance radiative interchange. The conduction path is through the aluminum housing. The actuator is adjusted relative to the frame to obtain the desired temperature

Table 9.1. Characteristics of Flight-Qualified Rectangular-Blade Louver Assemblies^a

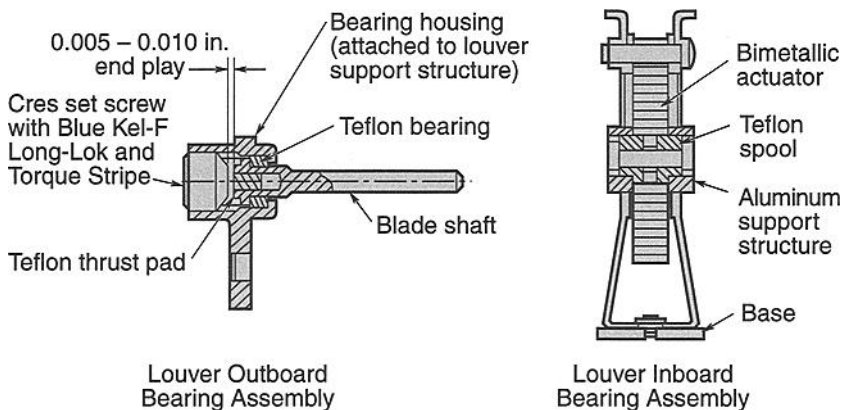
	OSC	Swales	Starsys
Blades	3 to 42		1 to 16
Open set points (°C)		0 to 40	-20 to 50
Open/close differential (°C)	10 or 18	10 or 18	14
Dimensions (cm)			
Length	20 to 110	27 to 80	8 to 43
Width	36 to 61	30 to 60	22 to 40
Height		6.4	6.4
Area (m ²)	0.07 to 0.6	0.08 to 0.5	0.02 to 0.2
Weight/area (kg/m ²) ^b	3.2 to 5.4	~ 4.5	5.2 to 11.6
Flight history	Nimbus, Landsat, OAO, ATS-6, Viking, GPS, SolarMax, AMPTE, SPARTAN, Hubble, Magellan, GRO, UARS, EUVE, TOPEX, GOES, MGS, MSP	XTE, Stardust	Rosetta ^c , Quickbird ^c JPL: ^d Mariner, Viking, Voyager, Galileo, MLS, Magellan, TOPEX, NSCAT, Cassini, Seawinds

^aThis table contains representative values from past louver designs. Contact manufacturer for additional design possibilities or values for specific designs.

^bWeight without sunshield.

^cLaunch to occur after date of handbook publication.

^dThe Starsys design is a slightly modified version of a JPL louver design that has flown on the indicated spacecraft.

**Fig. 9.2. Louver bearing assemblies.**

range between fully closed and fully open positions. Each blade is supported inboard and outboard by a bearing assembly (see Fig. 9.2). Inboard, the Teflon spool bears against and rotates with respect to the aluminum support structure. The outboard end of the louver-blade shaft rotates within and is supported by a Teflon bearing, with end play established by the distance between the Teflon thrust pad and the set screw. Each louver blade consists of a central torque tube bonded to flanges. The louver-blade cross section forms a hollow, thin-walled rectangle of high aspect ratio. The blades are highly polished to reduce emittance.

Louver assemblies of the type described above have been used in satellite applications where direct solar illumination is generally avoided, such as Pegasus, the Orbiting Astronomical Observatory, NIMBUS, the Earth Resources Technology Satellite, Voyager, Seasat, and the Global Positioning System (GPS). Each louver assembly contains several independently actuated blades, so a degree of redundancy is inherent in this design approach.

An old RCA design approach employs active control of blade position through a bimetal/heater assembly (Fig. 9.3). Frame structures are used for the larger louver

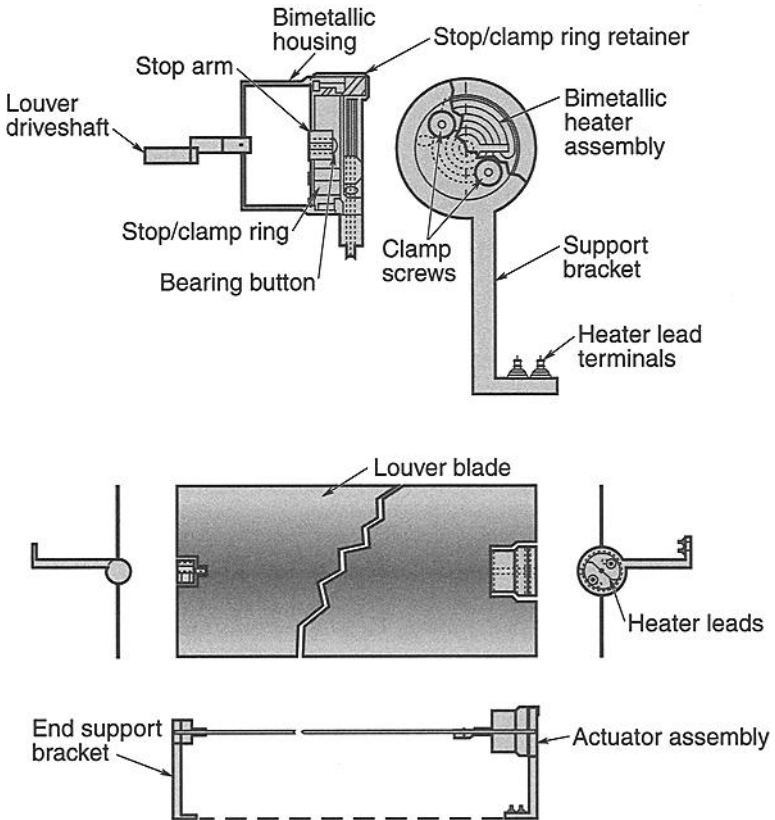


Fig. 9.3. Lockheed Martin louver assembly.

assemblies, while the smaller assemblies are frameless. In the latter case, the actuator and the end-support bracket are aligned and then attached to the equipment mounting plate with a foamed closeout used at the edges. The blades are supported and centered inboard by the bimetal/heater assembly. The fiberglass shaft with bonded-on, ball-end pivot is supported outboard by a Delrin AF bushing in the end-support bracket. The blades, composed of a foam sandwich about the fiberglass quill, have a 1-mil, first-surface-aluminized Kapton film on each side.

The bimetal/heater assembly drives the blade from fully closed to fully open over only a 1°C temperature change. The louver begins to open passively (by conduction from the mounting plate to the bimetallic spring) at about 10°C. This passive opening provides backup if the active controller fails off. The failed-on case can be corrected by ground disabling of the heater circuit. The bearing/support system provides a load-carrying capability during ground testing and, if alignment is true, the absence of friction on-orbit.

Analysis of Vane Louvers

Heat-Transfer Characteristics

Radiation through louvers is characterized by an effective emissivity ϵ_{eff} and an effective absorptivity α_{eff} that satisfy the steady-state energy equation for an isothermal body in a solar-space environment:

$$\frac{\dot{Q}}{A} = \epsilon_{\text{eff}}\sigma T^4 - \alpha_{\text{eff}}S, \quad (9.1)$$

where \dot{Q} (W) is the net heat transfer from louvered area A (m^2), σ is the Stefan-Boltzmann constant ($5.668 \times 10^{-8} \text{ W/m}^2 \cdot \text{K}^4$), T (K) is the absolute temperature, and S (W/m^2) is the solar constant.

Effective Emissivity

Effective emissivity is the ratio of net heat transfer from a louvered surface to the radiation from an equivalent black area ($\epsilon = 1.0$) at the same temperature but without louvers. When no external heat sources are present, the definition reduces to

$$\epsilon_{\text{eff}} = \frac{\dot{Q}}{A\sigma T^4}. \quad (9.2)$$

Equation (9.2) is written in this form to express a simplified equivalence to gray-body radiation. Actual heat transfer in louvered systems involves conduction along the frame and actuator housing cover, heat loss through actuator insulation and blade shafts, and variable feedback from reflections off the specular blades. In addition, friction effects are inconsistent and generally result in nonuniformity in the blades' angular positions. Effective-emissivity test values obtained by Eq. (9.2) will inherently contain these distortions and other deviations from the values associated with a purely radiative system.

Effective-emissivity tests are conducted in a cryogenic vacuum chamber.^{9.1,9.2} A louvered panel is instrumented with heaters and thermocouples; its unlouvered

back side is covered by multilayer insulation (MLI) and guard heaters. This setup practically eliminates radiation from the back and provides more accurate estimates of the amount of energy escaping through the louvers. The assembly is suspended in the chamber by low-conducting wires, and a series of steady-state temperatures are recorded corresponding to various heater power levels. Effective emissivity is calculated from the data via Eq. (9.2).

Some test results are shown in Fig. 9.4, with additional data in Table 9.2. All panels in the tests were uniformly heated and maintained nearly isothermal. The data were adjusted to account for a vacuum-chamber wall temperature higher than absolute zero (usually -190°C).

Friction effects are thought to account for the discrepancy between the values of effective emissivity obtained as equilibrium is approached from above versus the values obtained when it is approached from below, but the test points in these graphs can generally be contained within two straight lines that bound the louver's performance. A linear variation between closed and open positions is commonly assumed in thermal analysis, thus

$$\epsilon_{\text{eff}} = \epsilon_c(\text{constant}), T \leq T_c \quad (9.3)$$

$$\epsilon_{\text{eff}} = \epsilon_o - \frac{\epsilon_o - \epsilon_c}{1 - T_c/T_o} (1 - T_c/T_o), T_c \leq T \leq T_o \quad (9.4)$$

$$\epsilon_{\text{eff}} = \epsilon_o(\text{constant}), T \geq T_o, \quad (9.5)$$

Table 9.2. Louver Effective Emissivity (Test Data)

Program Louver Size (cm)	Radiator Hemispherical Emittance	ϵ_{eff}		Radiator ^a ΔT (K)
		Open	Closed	
ATS-6 ^b 45.7 × 58.2	OSR $\epsilon = 0.77$	0.62	0.114	18.0
ATS-6 45.7 × 58.2	Z-306 $\epsilon = 0.88$	0.71	0.115	18.6
GPS 40.6 × 40.5	Z-306 $\epsilon = 0.88$	0.70	0.090	18.0
Intelsat CRL ^c 62.2 × 60.5	AgTEF $\epsilon = 0.76$	0.67	0.080	10.0
MMS Landsat-4 ^d 55.6 × 108.1	Z-306 $\epsilon = 0.88$	0.39	0.100	17.0

^a $\Delta T = T(\text{open}) - T(\text{closed})$. In vacuum there is usually about a 2°C lag between radiator temperature and bimetallic temperature.

^bATS-6 has white stripes on the louver blades and a fiberglass actuator housing treated with aluminized Kapton tape (Kapton out).

^cCounterrotating blades ATS-6 housing and blades and enlarged springs.

^dAluminum shield with AgTEF exterior and Z-306 painted interior.

where the subscripts o and c refer to fully open and fully closed positions. A quadratic form of this equation sometimes more accurately represents temperature dependence in the active region:

$$\epsilon_{\text{eff}} = \epsilon_o - \frac{\epsilon_o - \epsilon_c}{(1 - T_c/T_o)^2} (1 - T/T_o)^2, T_c \leq T \leq T_o \quad (9.6)$$

Analysis shows variations that can be represented by segments of sine or cosine curves.^{9,3,9,4} This variation is an expected result of the idealized mathematical models that incorporate assumptions of infinite blade length and heat transfer only by radiation. Under those assumptions, effective emissivity varies almost linearly with projected open area, which is a trigonometric function of blade angle.

Equation (9.2) is also used to calculate from test data the effective emissivity of a shielded louver, F_ϵ . Theoretically, F_ϵ is related to ϵ_{eff} (effective emissivity of a louver without a shield) by the equation

$$F_\epsilon = \frac{\epsilon_i \epsilon_{\text{eff}}}{\epsilon_{\text{eff}} \epsilon_i + \epsilon_e} \quad (9.7)$$

where ϵ_i and ϵ_e are internal (facing the louver) and external emissivities of the shield. Since test values include conduction and other forms of heat loss, they are found to be slightly higher than the theoretical values obtained via Eq. (9.5).

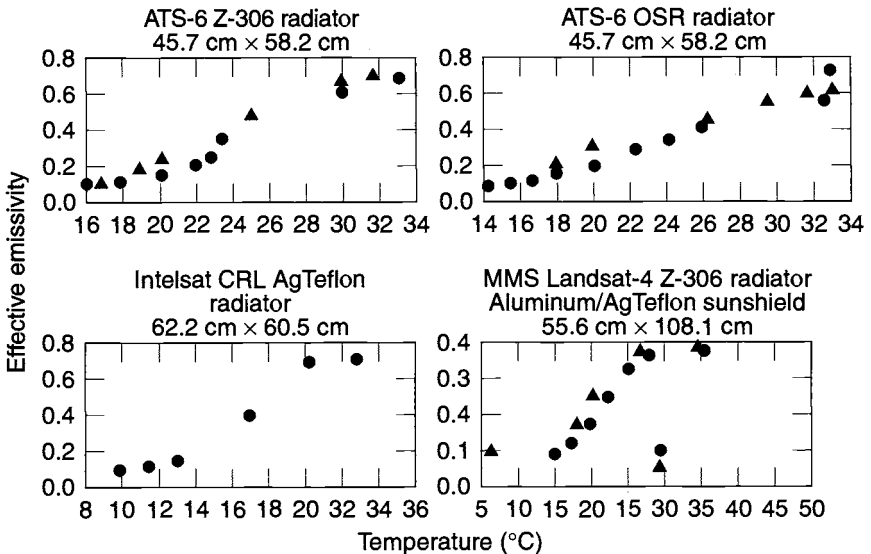


Fig. 9.4. The variation of louvers' effective emissivity with temperature (test data).

Effective Absorptivity

Effective solar absorptivity of a louvered panel may be defined as the fraction of incident solar energy absorbed per unit area of a louvered surface. The definition appears in Eq. (9.1) as

$$\alpha_{\text{eff}} = \frac{\epsilon_{\text{eff}} \sigma T^4 - \dot{Q}/A}{S} \quad (9.8)$$

where, again, \dot{Q} is actual net heat loss by a louvered surface having area A . The impinging solar flux S (nominally 1350 W/m^2 in Earth orbit) is not modified by the direction cosines, so the values of α_{eff} inherently contain the effects of solar multireflection off specular components.

Equation (9.6) is used to obtain the effective absorptivity by testing. The test configuration used for finding ϵ_{eff} is modified to include a sun simulator and a means of varying the angle of incidence. A detailed description of a typical facility is given in Michalek, Stipandic, and Coyle.^{9.1}

Few solar-simulation tests have been performed on louvers to date, and published data remain scanty. The results of tests on two early versions of the type eventually used in the ATS-6 program are reported in Michalek, Stipandic, and Coyle.^{9.1} These units, however, did not have many of the design features later added to enhance thermal performance, and the results differ somewhat from those obtained with later louvers. Data from two sets of louvers that represent current designs are given in Fig. 9.5. The effective absorptivity was calculated using Eq. (9.6), with effective emissivity (as a function of fixed-blade angle) already known from tests without solar input. The tests were conducted in solar-simulation chambers using xenon compact-arc-type lamps with a beam half-angle collimation of less than 1.5 deg . The mounting radiators were uniformly heated and

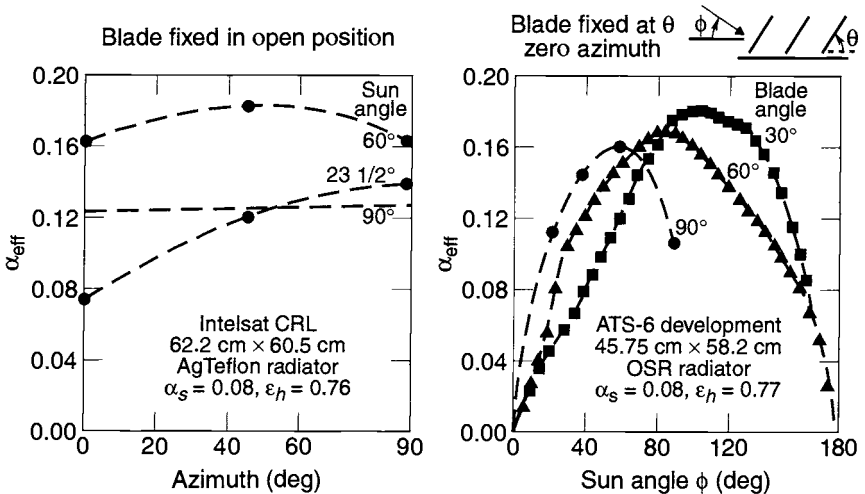


Fig. 9.5. Louver effective solar absorptivity variation with azimuth and blade angle (test data).

were sufficiently conductive (1.27-cm-thick aluminum) to limit lateral gradients to less than 2°C. All data were obtained shortly after application of radiator coating and hence are undegraded values. For long-term performance evaluation, and at least for fully open louvers, the practice has been to increase the values of ϵ_{eff} by the ratio of the radiator's estimated degraded absorptivity to the as-applied value.

Experimental data on the trend of variation of effective absorptivity with blade angle at zero azimuth agree reasonably well with analysis.^{9,3,9.1} Correlation with the predicted values is also good when the mathematical models incorporate the gap between the blade louver edge and the mounting panel.^{9.5} However, for azimuths other than zero, correlation becomes erratic, particularly at blade angles less than fully open. The major reasons for this irregularity probably lie in falsely assuming during analysis that the blades are infinitely long (length-to-width ratio of a blade is generally less than 5.0) and in ignoring the presence of the frame and the actuator assembly.

Effective absorptivity is not defined for shielded, louvered radiators. An efficient sun-shield design requires a low-solar-absorptance, high-emittance coating on the exterior. The interior surface should have high emittance to enhance heat exchange with the radiator when the blades are open. In cases where spacecraft envelopes permit, an oversized shield of potentially very low temperature should be considered.

Performance Curves

Performance curves of louvered radiators relate the heat-rejection rate to the radiator temperature. The curves are usually generated for steady-state, isothermal conditions in order to reflect maximum and minimum heat-rejection capabilities. This information is used in the initial phase of development of a thermal design to determine a louver size that will accommodate the required heat-rejection rates at specified temperatures and environment.

Equation (9.1) can be modified to include heat inputs from infrared (IR) sources (such as Earth) and reflected solar energy (albedo):

$$\frac{\dot{Q}}{A} = \epsilon_{\text{eff}}(\sigma T^4 - I) + \alpha_r f S - \alpha_{\text{eff}} S \quad (9.9)$$

Here I is infrared and $\alpha_r f S$ (f is the albedo factor) is reflected solar energy (usually diffuse), which filters through the louver and is absorbed by the radiator with solar absorptance α_r . In practice, a lack of experimental and flight data results in uncertainty in including this effect. One approach is to modify incident albedo by the effective emissivity before multiplying by α_r . This technique adjusts the diffuse input, in a sense, by a view factor prior to impingement on the radiator. A more conventional but conservative approach is to replace α_r by α_{eff} .

The effective emissivity, ϵ_{eff} , in Eq. (9.7) implicitly contains the radiator emissivity and is a predetermined function of radiator temperature. Effective absorptivity is assumed to be a known function of blade angle (which is linearly related to temperature) and sun angle. IR radiation, as it appears in Eq. (9.7), is the value adjusted by view factors to an imaginary louver plane parallel to the radiator. Incident

solar flux, S , is not modified by the angle of incidence, in conformity with the definition of α_{eff} .

Net heat rejected from a shielded louvered surface is obtained from the equation

$$\frac{\dot{Q}}{A} = F_e \left\{ \sigma T^4 - \left[\frac{\alpha_e}{\epsilon_e} S (\sin \theta + f) + I \right] \right\}, \quad (9.10)$$

where θ is the sun incident angle and the subscript e refers to the exterior of the shield. IR flux is adjusted by script-F from sources to shield.

For many satellite systems, the performance of louvered radiators may be evaluated by considering net heat rejection averaged over an orbital period. In this approach Eqs. (9.7) and (9.8) become very useful. This averaging technique has been found valid for many thermal designs in which massive electronic components are mounted to a louvered honeycomb tray.^{9,6,9,7}

Shielded vs. Unshielded Louvers: Special Cases

In a louvered design, maximum heat rejection must occur in the open-blade position, while only negligible heat should be transferred when the blades are closed. While the mere presence of louvers will inevitably lead to some radiation blockage with open blades, the situation can be improved by making the thicknesses of blades and frame and the width of the actuator housing as small as is practical, and by providing a highly reflective finish on the surfaces viewed by the radiator. But, as noted earlier, the specularity of louver parts leads to sun-ray entrapment and a reduction in heat rejection. Shielding will eliminate this effect, at the expense of introducing an additional resistance to radiation to space.

In the following special cases, a comparison is made between the hot-case operations (open louvers) of shielded and unshielded louvers based on orbital average performance under various environments. The shielded system is assumed to be a configuration of the Multimission Modular Spacecraft (MMS) type, with the following characteristics:

- Sun shield $\alpha_e = 0.14$
- Sun shield $\epsilon_e = 0.76$
- Sun shield $\epsilon_t = 0.88$
- Radiator $\epsilon_r = 0.88$
- Effective emissivity without shield $\epsilon_{\text{eff}} = 0.71$
- Effective emissivity with shield (Eq. [9.5]) $F_e = 0.34$

The properties of the unshielded system are assumed to be those of the Intelsat counterrotating louver (CRL), with effective emissivity of 0.67 and effective absorptivity as described in Fig. 9.5. In the calculations, the solar constant was taken as 1350 W/m^2 , albedo factor 0.35, and Earth radiation 200 W/m^2 .

Solar and Albedo Equal Zero

For satellites where louvers are mounted on shadowed or antisun sides having negligible albedo input, heat rejection is

$$\left(\frac{\dot{Q}}{A}\right)_{\text{unshielded}} = \epsilon_{\text{eff}}(\sigma T^4 - I) \quad (9.11)$$

$$\left(\frac{\dot{Q}}{A}\right)_{\text{shielded}} = F_e(\sigma T^4 - I) \quad (9.12)$$

Since for the given data ϵ_{eff} is nearly twice F_e in the open position ($\epsilon_{\text{eff}} \sim F_e$ in the closed position), unshielded louvers are much preferred in a purely IR environment. The orbital average-heat rejection as a function of radiator temperature is given in Fig. 9.6. An I value of 200 W/m^2 corresponds to Earth-flux input in a low-altitude orbit. The case $I = 0$ corresponds to a geosynchronous orbit with perfectly aligned north and south faces.

Sun-Oriented Low Earth Orbit

A similar comparison can be made for a spacecraft that is sun-oriented in a 370-km, 30-deg-inclined orbit. Two orientations are considered: the first, shown in Fig. 9.7, is such that the sun vector is parallel to the open louver blades during the sun-light portion of the orbit; in the second, shown in Fig. 9.8, the sun vector is inclined 30 deg off the normal to the plane of the louver. The second orientation represents the maximum solar input to an open louver array as indicated in Fig. 9.5. The graphs in Figs. 9.7 and 9.8 illustrate that the orbital average heat rejection is greater for unshielded louvers in both cases.

Earth-Oriented Low Earth Orbit

A condition in which the combined absorbed solar and Earth flux is maximum during a near-Earth polar orbit is given in Fig. 9.9. In this case, the sum of the Earth- and solar-flux inputs to exposed louvered radiators is relatively large and remains nearly constant when the angle between the sun and the plane of the louvers varies between 30 deg and 60 deg. At smaller angles, close to 30 deg, heating

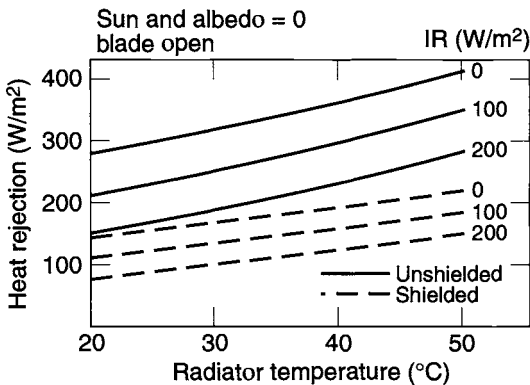


Fig. 9.6. Louver heat rejection in IR environment.

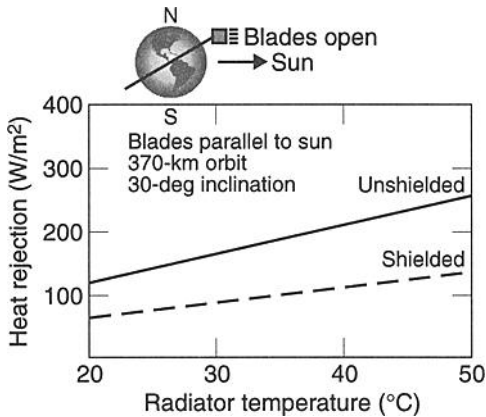


Fig. 9.7. Shielded vs. unshielded louvers in sun-oriented near Earth orbit, sun parallel to blades.

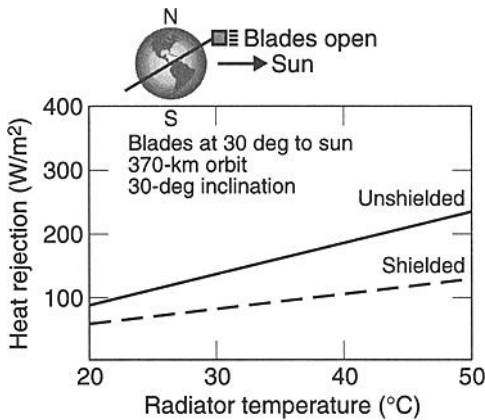


Fig. 9.8. Shielded vs. unshielded louvers in sun-oriented near Earth orbit, sun at 30 deg to blades.

from the Earth represents about 50% of the total absorbed input. At larger angles, although Earth flux diminishes, solar flux increases. In this particular orbit, the exposed louver system can exhibit less heat rejection capability than a shielded configuration. A change in the orbit hour, however, equivalent to a rotation of the plane of the orbit, introduces a shadow period that reduces the net solar input so that, even for short shadow time, exposed louvers are more efficient on an orbital average basis. The crossover point depends on radiator temperature. For 30°C it is shortly after 8 hours.

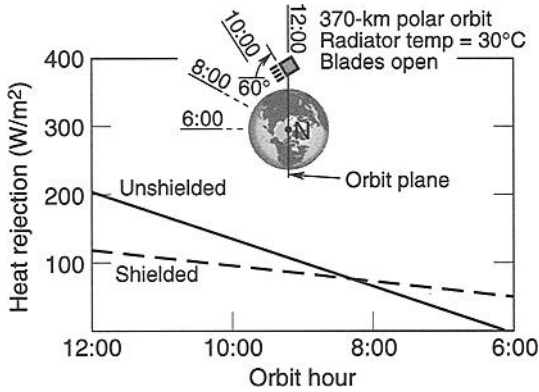


Fig. 9.9. Shielded vs. unshielded louvers in near-Earth polar orbit, louver blades at 60 deg to orbit plane.

Earth-Oriented Geosynchronous Orbit (No Shadow)

Consider an Earth-oriented geosynchronous orbit during which the solar vector moves at various angles inclined to the plane of the louver. The effective absorptivity for exposed louvers varies continuously with azimuth, as shown in Fig. 9.5. The orbital average value of α_{eff} for open blades (Table 9.3) at a given sun angle can be calculated from CRL test data.

Figure 9.10 shows heat rejection plotted as a function of radiator temperature for no-shadow periods. Even under the worst heating angles, unshielded louvers are more efficient than shielded ones at the radiator temperatures usually encountered in spacecraft temperature control.

This study shows that an exposed louver system offers greater heat rejection in most practical cases. An exception is a near-Earth orbit in which the louver continuously views the sun 30-deg to 60-deg off normal. Of course, other orbits and trajectories are possible, and comparison studies must include orbital transient variations. But with the introduction of even small shadow periods, most systems exhibit greater heat-rejection rates when the louvers are exposed.

Table 9.3. Orbital Average Value of Effective Absorptivity for Exposed Louvers

Sun Angle (deg)	Orbit Average α_{eff}
0.0	≈0.0
23.5	0.109
60.0	0.178
90.0	0.124

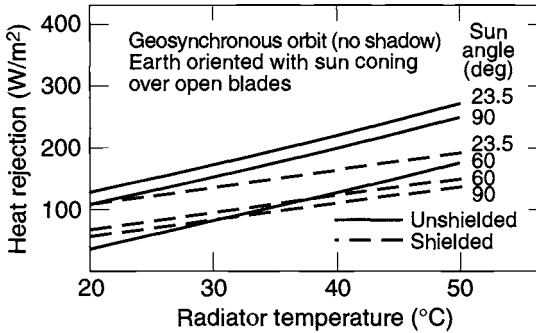


Fig. 9.10. Shielded vs. unshielded louvers in Earth-oriented geosynchronous orbit.

Louver Transient Response

In most applications, louvers are mounted to equipment baseplates with large thermal masses. Hence the orbital temperature change of radiators is generally not radical, and bimetallic response follows closely.

Actuator response time may be quantified by considering hypothetical cases in which an instantaneous step change in radiator temperature occurs. Response time can then be characterized by the time required for a louver to complete a half cycle, from fully closed to fully open or vice versa.

The transient problem is usually treated by constructing a small nodal model with conduction coupling between the radiator and the actuator housing and radiation couplings between the radiator, the actuator, and the external environment. There is significant sensitivity of response time to the values of conductances, and it may become necessary to conduct simulation tests if response time is a critical factor in predicting performance.

Typical profiles are given in Figs. 9.11 and 9.12. These graphs represent the results of analysis of shielded louvers in a near-Earth high-noon orbit. The mounting flange of the actuator housing was assumed to contact the radiator with an interface conductance of $140 \text{ W/m}^2\text{-K}$. The actuators were radiatively coupled to the inner structure of the housing, which is coupled to the exterior structure through the surrounding MLI. The effective emissivity of the louver was assumed to vary linearly between 0.115 (at 10°C) and 0.70 (at 28°C). The actuator temperature reaches the value for which the louver opens or closes in approximately 24 minutes.

Nonisothermal Transient Analysis

Thermal analysis of nonisothermal and transient radiators is performed by resorting to nodal computer models.^{9.7} A typical arrangement is shown in Fig. 9.13. The nodes labeled 1 through 6 are located immediately facing the actuators and are thermally coupled to them. The temperatures of nodes 1 through 6 are used to determine the emissivity values of the other louver nodes with respect to their location within blade pairs or within a blade and an end frame. For example, the temperature of nodal point 1 sets the emissivity value of 7 and 8 in accordance

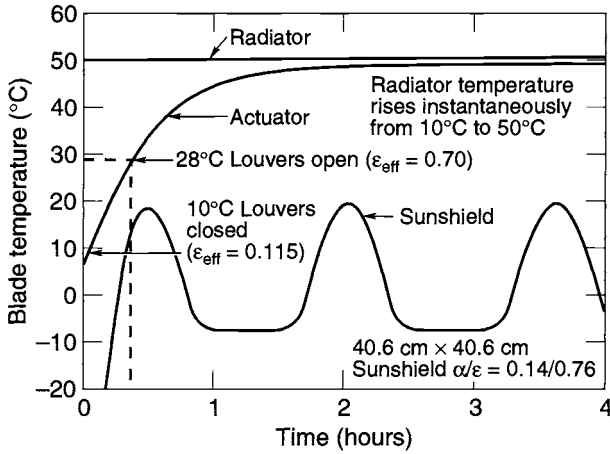


Fig. 9.11. Louver heat-up response (450-km noon orbit).

with a given temperature-emissivity matrix. The input data file may also contain the effective absorptivity as a function of sun angle (in plane ψ and azimuth ϕ) and blade angle θ , or temperature.

For exposed louvers, the quasi-steady-state equation

$$\frac{\dot{Q}}{A} = \epsilon_{\text{eff}}(\theta)[\sigma T^4 - I] - \alpha_r(\theta)fS - \alpha_{\text{eff}}(\psi, \phi, \theta)S \quad (9.13)$$

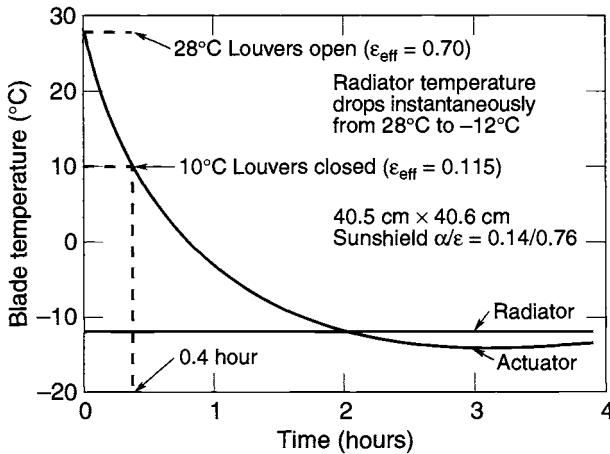


Fig. 9.12. Louver cool-down response (450-km noon orbit).

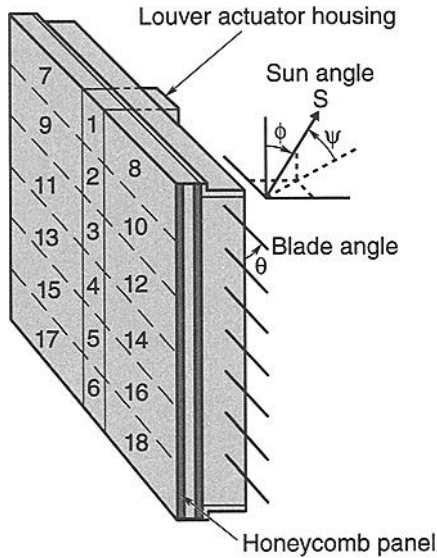


Fig. 9.13. Nodal model of a louvered panel.

is used with applicable orbital parameters to generate values of Q as a function of T (or θ) and (ψ, ϕ) . The values are tabulated as bivariate arrays and input to the transient thermal model (usually in SINDA format). The computer program performs a first interpolation using orbit position (time) to select for each θ the appropriate T and Q array. A second interpolation, made using the value of sun angles, calculates heat rejected at a particular nodal point. The double interpolation for each node can require lengthy computer time, and consideration may be given to generating orbital average (steady-state) data for approximate representation of actual behavior.

Shielded louvered radiators are similarly modeled with nodes on the shield corresponding, in a one-to-one radiation coupling, to opposing nodes on the radiator. Cross-viewing among nodes does not generally exist, because of the close proximity of louver blades and shield.

An analytical treatment of nonisothermal louvered radiators is presented in Karam.^{9,8} An important conclusion from that study is that the usual profiles of effective emissivity vs. temperature, generated for isothermal panels, apply in nonisothermal systems, provided that the distance between centers of adjacent blades is not too large. Another conclusion is that the use of louvers leads to significant reduction in potential lateral gradients.

Designing Louvers for Operation in Sunlight

As shown earlier, trapping of sunlight between louver blades can reduce the efficiency of louvered radiators by increasing their effective solar absorptance. While pinwheel louvers and sun-shielded vane-type louvers eliminate solar trapping,

they have inherently lower heat-rejection capability per unit area. Therefore, in some circumstances, a louver designed to operate with direct solar illumination proves to be the best alternative. Successful operation in a solar environment requires isolation of the actuator from solar heating, avoidance of material or bond degradation from overheating, and an increase in radiator area to compensate for the trapped solar heat load. Swales and Orbital Sciences make louvers designed for unshielded operation under solar loads in Earth orbit, and JPL has designed (and licensed to Starsys) a louver capable of solar exposure at up to 2.7 solar constants.

Available test data on louvers in sunlight confirm the prediction that high temperatures can be reached on the blades.^{9,4} This condition presents problems of outgassing and delamination in designs where adhesives are used to bond plate sections. In addition, conduction-heat transfer from heated blades can reduce the long-term reliability of the bearings and actuator spool.

The temperature may be lowered by introducing strips of white paint (low absorptivity and high emissivity) on the blade surfaces. The equivalent absorptance-to-emittance ratio is thus reduced, leading to cooler temperatures. This effect is apparent in Fig. 9.14, a graph that depicts the results obtained in research at NASA Goddard Space Flight Center. The graph in Fig. 9.15 shows how blade temperature can relate to the percentage of blade surface area (one side) that is painted. Standard applications limit the amount to about 15%, and the stripes are usually located near the blade edge that is farthest from the radiator with the white exposed when the blades are closed. The effect of increased blade emissivity on effective emissivity is shown in Fig. 9.16.

Orbital Sciences' high-temperature louver assembly employs an insulated housing, blade white-striping to reduce blade temperature, a Vespel shaft to isolate the actuators from blades having a maximum predicted temperature of 220°C, and a silvered Teflon second-surface tape over the base. The JPL/Starsys design (Fig. 9.17) uses spot-welded blades riveted to the shaft for high-temperature mechanical integrity, a titanium shaft for high-temperature strength and low conductance,

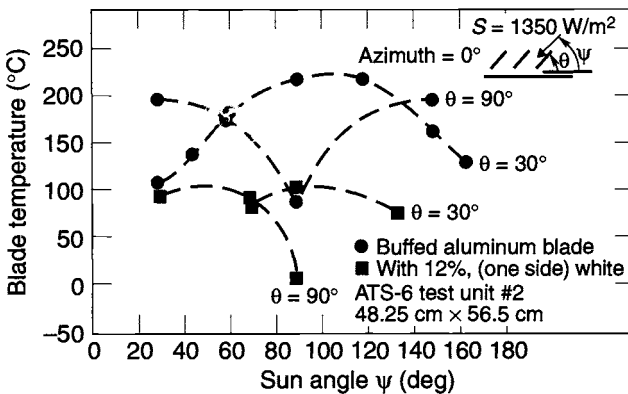


Fig. 9.14. Louver-blade temperature in the sun (test data).

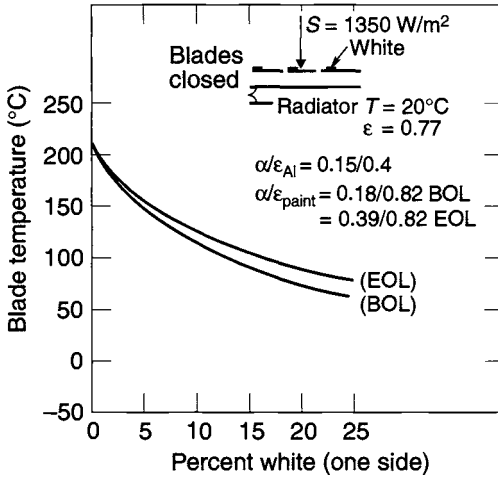


Fig. 9.15. Effect of white paint on blade temperature.

and a steel stop lever keyed to the main shaft that prevents deformation of the blade as a result of mechanical loads induced when the blades are driven open against the stop-pin at high temperature. This design can withstand the 370°C temperatures expected for partially opened blades and the 350°C expected for fully opened blades under the 2.7 solar constant illumination at 0.61 AU from the sun. One of the most important lessons learned in the development of this louver was that the bearing assembly had to accommodate the 1.5 mm of blade expansion that occurs at high temperature.

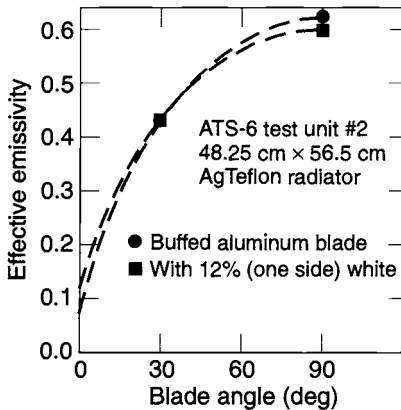


Fig. 9.16. Effect of painted blades on effective emissivity (test data).

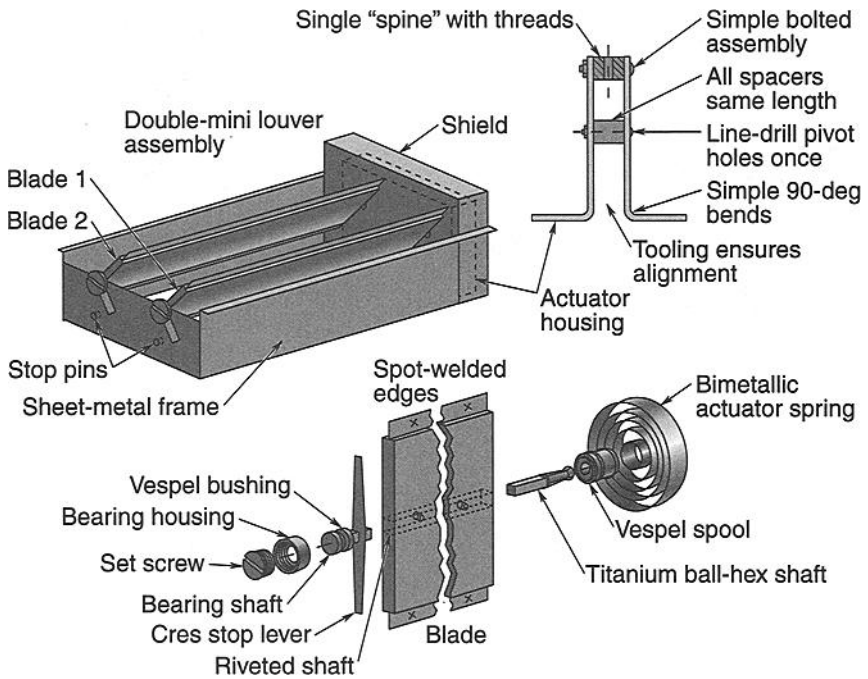


Fig. 9.17. JPL high-temperature louver.

Pinwheel Louvers

The pinwheel louver consists of a lobed louver blade, an actuator assembly, a guard ring, and a special radiator pattern, as shown in Fig. 9.18. This type of louver may be selected because of its low mechanical profile (it is less than 1.28 cm tall) or its tolerance of solar loads. The louver opens passively through the action of a bimetallic spring or is driven open by an electronic controller and a small heater on the spring. When fully open, however, the radiator surface constitutes only 5% of the circular area. An old RCA pinwheel louver-blade design, shown in detail in Fig. 9.19, consists of a fiberglass hub, foam sandwich blades, a fiberglass support framework, and a single aluminized-Kapton-film outer shield. The latter shields the hub and blades from most of the external environment. This protection is necessary to prevent wide variations in hub and blade temperatures, which would affect the bimetal temperature and thus its response.

The pinwheel actuator assembly is shown in detail in Fig. 9.20. It consists of a bimetallic element, bimetallic heater strip, driveshaft assembly, bimetallic housing, outer housing, clamp ring, stop element, and two Delrin AF bushings. The bimetallic heater strip is bonded directly to the bimetallic element, which in turn is bonded into the bimetallic housing.

The driveshaft assembly is attached to the inner coil of the bimetallic element and carries the stop arm and two bearing surfaces that ride in the Delrin AF bushings, one of which is mounted in the bimetallic housing. The bimetallic housing

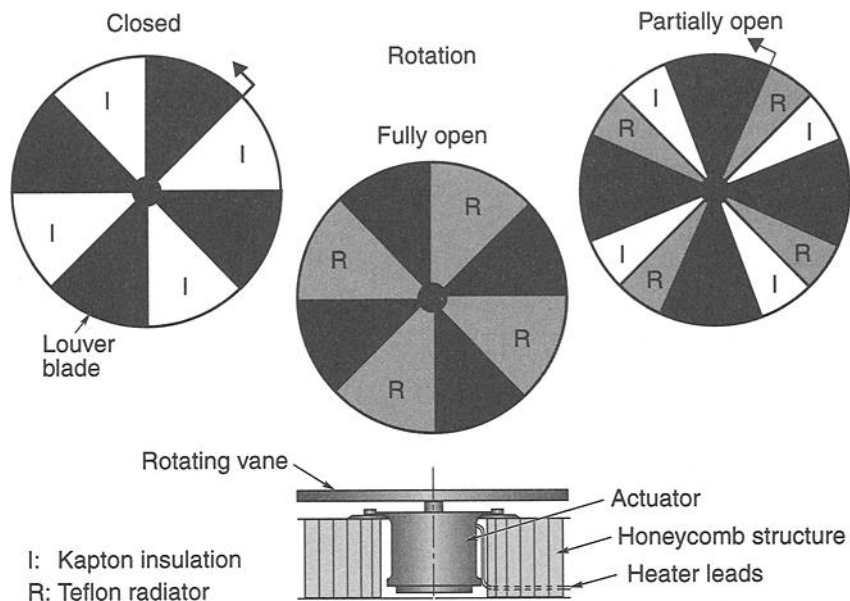


Fig. 9.18. Pinwheel thermal louver.

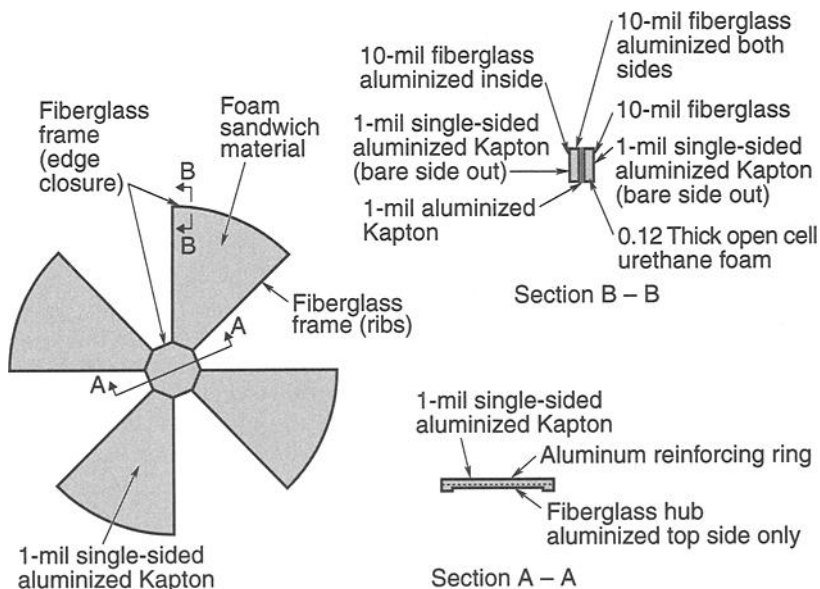


Fig. 9.19. Pinwheel louver blade.

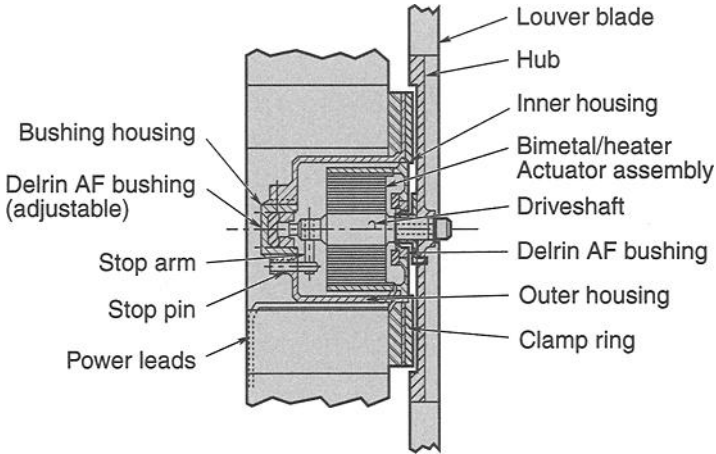


Fig. 9.20. Pinwheel louver actuator.

mounts inside the outer housing, which contains the stop element and an adjustable Delrin AF bushing. The whole assembly mounts in a hole in the spacecraft honeycomb-panel external wall and is held in place with a clamp ring. The actuator passive set point is adjusted by loosening the clamp ring, rotating the bimetallic housing, then retightening the clamp ring.

The stop elements limit the blade rotation at the fully closed and fully open positions (45 deg of angular rotation). The actuator operation is the same as for a vane louver actuator. A temperature change of 15°C is required to drive the louver from the fully closed position to fully open.

The Delrin AF bushings are adjusted at assembly to limit the driveshaft axial movement to 10 mils. They also provide low-torque louver-blade support during 1-g testing; this support minimizes the 1-g testing error.

The radiator/guard-ring assembly is shown in detail in Fig. 9.21. The radiator consists of a guard ring for louver-blade protection and alternating radiator segments of second-surface aluminized Teflon and aluminized Kapton. The Teflon areas are the radiating areas and have a low solar-absorptance value ($\alpha < 0.2$). The aluminized Kapton areas are the low emittance areas, which act as insulation when the louvers are closed. The louver blade covers the Teflon areas when in the closed position and the Kapton areas when in the open position.

Each RCA pinwheel louver had a heat-rejection capacity of approximately 25 to 30 W when open and a heat leakage of approximately 5 to 7 W when closed. The heat-rejection rate is linearly proportional to the louver-blade position.

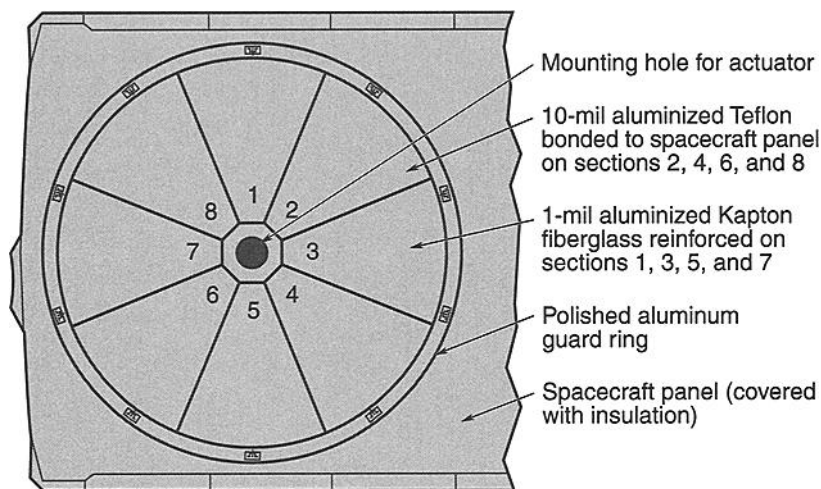


Fig. 9.21. Pinwheel louver radiator/guard ring assembly.

References

- 9.1. T. J. Michalek, E. A. Stipandic, and M. J. Coyle, "Analytical and Experimental Studies of an All Specular Thermal Control Louver System in a Solar Thermal Vacuum Environment," AIAA Paper 72-268 (1972).
- 9.2. W. H. Kelly, J. H. Reisenweber, and H. W. Fliieger, "High Performance Thermal Louver Development," AIAA Paper 76-460 (1976).
- 9.3. M. Furukawa, "Analytical Studies on Design Optimization of Movable Louvers for Space Use," *Journal of Spacecraft and Rockets* **16**, 412-425 (Nov.-Dec. 1979).
- 9.4. J. A. Plamondon, "Analysis of Movable Louvers for Temperature Control," *Journal of Spacecraft and Rockets* **1**, 492-497 (Sept.-Oct. 1964).
- 9.5. COMSAT Louver Thermal Analysis for INTELSAT, Fairchild Space Company Report No. 310-SR-2001 (with appendix) (May 1975).
- 9.6. R. O. Wales, ed., "ATS-6 Final Engineering Performance Report," Vol. I, NASA Reference Publication 1080 (Nov. 1981).
- 9.7. H. Hwangbo, J. H. Hunter, and W. H. Kelly, "Analytical Modeling of Spacecraft with Heat Pipes and Louvers," AIAA Paper 73-773 (1973).
- 9.8. R. D. Karam, "Temperature Distribution in Louvered Panels," *Journal of Spacecraft and Rockets* **16**, 92-97 (March-April 1979).
- 9.9. H. Frankel and R. Eby, "SMM Hardware Evaluation," Proceedings of the SMRM Degradation Study Workshop, NASA Document 408-SMRM-79-0001 (May 9-10, 1985), pp. 105-123.
- 9.10. A. J. Boscia, "A Laboratory Method for the Determination of Effective Emittance of Spacecraft Thermal Control Louvers," Joint National Meeting of American Astronautical Society (15th Annual) and Operations Research Society (35th National), (Denver, CO, June 17-20, 1969) Paper No. VIC. 3.
- 9.11. Design Catalog, Chase Thermostatic Metals, GTE Metal Laminates Division, 1704 Barnes Street, Reidsville, NC 27320.